

# A phase equilibrium model for atmospheric aerosols containing inorganic electrolytes and organic compounds (UHAERO), with application to dicarboxylic acids

N. R. Amundson,<sup>1</sup> A. Caboussat,<sup>1</sup> J. W. He,<sup>1</sup> A. V. Martynenko,<sup>1</sup> and J. H. Seinfeld<sup>2</sup>

## Abstract.

Computation of phase and chemical equilibria of water-organic-inorganic mixtures is of significant interest in atmospheric aerosol modeling. A new version of the phase partitioning model, named UHAERO, is presented here, which allows one to compute the phase behavior for atmospheric aerosols containing inorganic electrolytes and organic compounds. The computational implementation of the model is based on standard minimization of the Gibbs free energy using a primal-dual method, coupled to a Newton iteration. Water uptake and deliquescence properties of mixtures of aqueous solutions of salts and dicarboxylic acids, including oxalic, malonic, succinic, glutaric, maleic, malic, or methyl succinic acids, are based on a hybrid thermodynamic approach for the modeling of activity coefficients [Clegg and Seinfeld [2006a, b]]. UHAERO currently considers ammonium salts and the neutralization of dicarboxylic acids and sulfuric acid. Phase diagrams for sulfate/ammonium/water/dicarboxylic acid systems are presented as a function of relative humidity at 298.15K over the complete space of compositions.

## 1. Introduction

Atmospheric aerosols are composed of a mixture of water, inorganic compounds, organic compounds, mineral dust, black carbon, etc. The inorganic constituents of atmospheric particles typically consist of electrolytes of ammonium, sodium, calcium, sulfate, nitrate, chloride, carbonate, potassium, magnesium, etc. The mixture of inorganic and organic constituents in atmospheric particles is complex, as the number of organic components is large. The presence of organic species in solution may substantially influence phase transitions of the deliquescence and efflorescence of salts with changes in relative humidity [Erdakos and Pankow [2004]]. Reciprocally, dissolved electrolytes can have appreciable effects on the solubility of organic components in solution, see Salcedo [2006] or Marcolli and Krieger [2006]. Therefore accounting for the influence of organic solutes in electrolyte mixtures is important in thermodynamic calculations.

Dicarboxylic acids are ubiquitous in atmospheric particles and their behavior is representative of organics soluble in water, see for instance Kawamura *et al.* [2003] or Yu *et al.* [2005]. Presented here is a phase equilibrium model for atmospheric aerosols containing inorganic electrolytes and organic species, with application to dicarboxylic acids: oxalic, malonic, succinic, glutaric, maleic, malic, or methyl succinic acids. The comprehensive mathematical model for mixed inorganic-organic atmospheric aerosols is capable of predicting phase stability and separation.

---

<sup>1</sup> Department of Mathematics, University of Houston, 4800 Calhoun Rd, Houston, TX 77204-3008, USA.

<sup>2</sup> Department of Chemical Engineering, California Institute of Technology, Pasadena, CA 91125, USA.

46 A variety of thermodynamic models have been devel-  
47 oped to predict pure inorganic gas-aerosol equilibrium:  
48 ADDEM *Topping et al.* [2005a, b], AIM and AIM2 *Clegg*  
49 *and Pitzer* [1992]; *Clegg et al.* [1992, 1998a, b]; *Weiler*  
50 *and Clegg* [2002], EQSAM, EQSAM2 and EQSAM3 *Met-*  
51 *zger et al.* [2002a, b, 2006]; *Trebs et al.* [2005]; *Met-*  
52 *zger et al.* [2006]; *Metzger and Lelieveld* [2007], EQUI-  
53 SOLV and EQUISOLV II *Jacobson et al.* [1996]; *Jacobson*  
54 [1999], GFEMN *Ansari and Pandis* [1999, 2000], HETV  
55 *Makar et al.* [2003], ISORROPIA and ISORROPIA2  
56 *Nenes et al.* [1998]; *Pilinis et al.* [2000]; *Fountoukis and*  
57 *Nenes* [2007], MARS-A *Binkowski and Shankar* [1995],  
58 MESA *Zaveri et al.* [2005a, b] SCAPE and SCAPE 2  
59 *Kim et al.* [1993a, b]; *Kim and Seinfeld* [1995]; *Meng*  
60 *et al.* [1995], UHAERO *Amundson et al.* [2006a] and the  
61 older thermodynamic models: EQUIL *Bassett and Seinf-*  
62 *feld* [1983], KEQUIL *Bassett and Seinfeld* [1984], MARS  
63 *Saxena et al.* [1986] and SEQUILIB *Pilinis and Seinfeld*  
64 [1987]. Some of these modules have been compared in  
65 *Zhang et al.* [2000] and *Amundson et al.* [2006a]. Predic-  
66 tion of the thermodynamic equilibrium for mixtures of  
67 inorganic and organic components has received less at-  
68 tention. Organics are currently considered for instance in  
69 the thermodynamic framework of ADDEM *Topping et al.*  
70 [2005b] and EQSAM3 *Metzger and Lelieveld* [2007]. The  
71 studies of *Trebs et al.* [2005]; *Metzger et al.* [2006]; *Clegg*  
72 *and Seinfeld* [2006a, b]; *Erdakos and Pankow* [2004] have  
73 demonstrated the importance of organic acids for the ion  
74 balance, which particularly affects the phase partitioning  
75 of (semi-)volatile compounds such as ammonia.

76 When predicting the thermodynamic equilibrium for  
77 mixtures of inorganic and organic components with a  
78 standard approach, hybrid methods are required for com-  
79 puting activity coefficients in inorganic/organic mixtures,  
80 which incorporate different models, and for which rele-  
81 vant experimental data are often not available. Also, the  
82 computation of the thermodynamic equilibrium requires  
83 advanced computational techniques that can be numeri-  
84 cally demanding.

85 In the following, a computational framework (UHAERO)  
86 for the determination of the thermodynamic equilibrium  
87 of a mixture of inorganic and organic compounds is pre-  
88 sented. In order to show the capabilities of UHAERO,  
89 a hybrid approach is used, namely the Pitzer-Simonson-  
90 Clegg (PSC) and UNIFAC activity coefficient models, to-  
91 gether with a CSB approach (*Clegg and Seinfeld* [2006b])  
92 for the modeling of interactions between inorganic elec-  
93 trolytes and organic dissociated components. It is flexible  
94 and can incorporate other models for the activity coeffi-  
95 cients.

96 A numerical technique for the efficient computation  
97 of the equilibrium is described in this article. One can  
98 calculate the composition of the aerosol either by solv-  
99 ing the set of nonlinear algebraic equations derived from  
100 mass balances and chemical equilibrium or by performing  
101 a direct minimization of the Gibbs free energy. Since di-  
102 rect minimization of the Gibbs free energy has tended to  
103 be computationally demanding (making its use in large-  
104 scale atmospheric models unattractive, since thermody-  
105 namic calculations are implemented in principle for each  
106 grid cell and at each time step), we propose an approach  
107 based on solving the governing set of nonlinear equations.  
108 This approach is an extension of the solution method pro-  
109 posed in *Amundson et al.* [2006a] for calculation of the  
110 equilibrium of systems containing inorganic species only.

111 The most challenging aspect of the numerical determi-  
112 nation of the equilibrium is the prediction of the parti-  
113 tioning of aerosol components between aqueous and solid  
114 phases. A number of current methods rely on *a priori*

115 specifications of the presence of certain phases at a cer-  
 116 tain relative humidity and overall composition. While  
 117 these assumptions may facilitate numerical determina-  
 118 tion of the equilibrium, they lead to approximations in  
 119 the phase diagram of the system that may be undesirable,  
 120 see *Ansari and Pandis* [1999].

121 What is ultimately needed is an efficient computa-  
 122 tional model for the equilibrium partitioning of inorganic  
 123 electrolytes and organic compounds between aqueous and  
 124 solid phases that does not rely on a priori knowledge of  
 125 the presence of certain phases at a given relative humid-  
 126 ity and overall composition. For the organic composition,  
 127 we focus here on dicarboxylic acids.

128 We present a new version of the phase partitioning  
 129 model for mixtures of inorganic electrolytes and dicar-  
 130 boxylic acids (UHAERO), which is an extension of the  
 131 inorganic atmospheric aerosol phase equilibrium model  
 132 presented in *Amundson et al.* [2006a].

133 The next section summarizes the standard minimiza-  
 134 tion problem; its mathematical foundation and computa-  
 135 tional implementation are presented in *Amundson et al.*  
 136 [2005, 2006b]. The following sections are devoted to  
 137 the modeling of the activity coefficients, the computa-  
 138 tional aspects of aerosol phase equilibria in the system  
 139 composed of sulfate, nitrate, water and a dicarboxylic  
 140 acid, and the simulation of such systems. Detailed phase  
 141 diagrams of the sulfate/ammonium/water/dicarboxylic  
 142 acid systems, including oxalic, malonic, succinic, glutaric,  
 143 maleic, malic, and methyl succinic acids, are presented as  
 144 a function of relative humidity at 298.15K over the com-  
 145 plete space of compositions.

## 2. Thermodynamic Equilibrium

146 The multicomponent chemical equilibrium for a closed  
 147 gas-aerosol system at constant temperature and pressure  
 148 and a specified elemental abundance is the solution to  
 149 the following problem arising from the minimization of  
 150 the Gibbs free energy,  $G$ ,

$$\min G(\vec{n}_l, \vec{n}_g, \vec{n}_s) = \vec{n}_g^T \vec{\mu}_g + \vec{n}_l^T \vec{\mu}_l + \vec{n}_s^T \vec{\mu}_s, \quad (1)$$

151 subject to  $\vec{n}_g > \vec{0}$ ,  $\vec{n}_l > \vec{0}$ ,  $\vec{n}_s \geq \vec{0}$ , and

$$A_g \vec{n}_g + A_l \vec{n}_l + A_s \vec{n}_s = \vec{b}, \quad (2)$$

152 where  $\vec{n}_g$ ,  $\vec{n}_l$ ,  $\vec{n}_s$  are the concentration vectors in gas, liq-  
 153 uid, and solid phases, respectively,  $\vec{\mu}_g$ ,  $\vec{\mu}_l$ ,  $\vec{\mu}_s$  are the  
 154 corresponding chemical potential vectors,  $A_g$ ,  $A_l$ ,  $A_s$   
 155 are the component-based formula matrices, and  $\vec{b}$  is the  
 156 component-based feed vector. Condition (2) expresses  
 157 the fact, for example, that in calculating the partition of  
 158 any chemical component (in electrolytes and/or organic  
 159 species) between aqueous and solid phases the total con-  
 160 centration is conserved, while maintaining a charge bal-  
 161 ance in solution.

162 The chemical potential vectors are given by

$$\vec{\mu}_g = \vec{\mu}_g^0 + RT \ln \vec{a}_g, \quad (3)$$

$$\vec{\mu}_l = \vec{\mu}_l^0 + RT \ln \vec{a}_l, \quad (4)$$

$$\vec{\mu}_s = \vec{\mu}_s^0, \quad (5)$$

163 where  $R$  is the universal gas constant,  $T$  is the system  
 164 temperature,  $\vec{\mu}_g^0$ ,  $\vec{\mu}_l^0$  and  $\vec{\mu}_s^0$  are the standard chemical  
 165 potentials of gas, liquid and solid species, respectively,  
 166 and  $\vec{a}_g$  and  $\vec{a}_l$  are the activity vectors of the gas and liq-

167 uid species. For ionic components the elements of the  
168 activity vector  $a_i$  are equal to  $\gamma_i m_i$ , where  $\gamma_i$  and  $m_i$   
169 are the activity coefficient and molality ( $\text{mol kg}^{-1}$  wa-  
170 ter), respectively, of component  $i$ . The water activity is  
171 denoted by  $a_w$ . The temperature dependence of the stan-  
172 dard state chemical potentials is reported in *Amundson*  
173 *et al.* [2006a]. Particle curvature effects are neglected,  
174 but can easily be incorporated in the model.

175 Equations (1)–(5) represent a constrained nonlinear  
176 minimization problem. The standard method for its so-  
177 lution is presented in Section 4.

### 3. Modeling of Activity Coefficients

178 The key issue in the equilibrium calculation when us-  
179 ing the standard approach based on activity models, is  
180 the estimation of the activity coefficients. For aqueous  
181 inorganic electrolyte solutions, the Pitzer molality-based  
182 model [*Pitzer* [1973, 1975]; *Pitzer and Mayorga* [1973]]  
183 has been widely used, but it is restricted to high  $RH$  re-  
184 gions where solute molalities are low. These restrictions  
185 on the concentrations have been relaxed with the Pitzer,  
186 Simonson, Clegg (PSC) mole fraction-based model (see  
187 *Clegg and Pitzer* [1992]; *Clegg et al.* [1992]).

188 On a mole fraction scale, the activity of component  $i$  is  
189 expressed as  $a_i = f_i x_i$ , where  $f_i$  is the mole fraction-based  
190 activity coefficient, and  $x_i$  is the mole fraction of species  
191  $i$ . The molality-based and mole fraction-based activity  
192 coefficients are related by  $f_i x_w = \gamma_i$ .

193 A number of methods exist for calculating the water  
194 activity  $a_w$ . The most widely used is the Zdanovskii-  
195 Stokes-Robinson (ZSR) mixing rule (*Clegg et al.* [2003],  
196 *Stokes and Robinson* [1966]), in which only data on bi-  
197 nary solute/water solutions are needed to predict the wa-  
198 ter content of a multicomponent mixture. A more accu-  
199 rate determination of the water content can be obtained  
200 using the solvent activity model of *Clegg et al.* [1998a, b],  
201 which includes interactions between solutes, in addition  
202 to those between the solutes and water; in this case, the  
203 water activity is calculated from  $a_w = f_w x_w$ .

204 The organic components can dissociate in the liquid  
205 phase and they can form solid salts with the inorganic  
206 electrolytes. The soluble organic compounds have effects  
207 on the water content of the aerosol, and their dissociation  
208 will also affect the aerosol pH. This generalization leads  
209 to an extension of the species  $\vec{n}_g, \vec{n}_l, \vec{n}_s$  in the gas, liquid  
210 and solid phases respectively. The interactions between  
211 dicarboxylic acids and inorganic components have to be  
212 modeled and the activity coefficients  $f_i$  have to incor-  
213 porate the organic dependencies, although data are not  
214 always available. Owing to the lack of data, the modeling  
215 of aqueous solutions containing both ions and uncharged  
216 solutes up to high concentrations (low equilibrium rela-  
217 tive humidity) is still quite approximate, see *e.g.* *Griffin*  
218 *et al.* [2005], *Pun et al.* [2002].

219 The *PSC model* (*Clegg et al.* [1998a, b]) for inorganic  
220 (electrolyte) multicomponent solutions and the *UNIFAC*  
221 *model* (*Fredenslund et al.* [1977]) for water/organic mix-  
222 tures, are combined in a self-consistent way to incorpo-  
223 rate the mutual influence of ions and organic molecules  
224 on the activities of all components. The water uptake  
225 and deliquescence properties of aqueous solutions of di-  
226 carboxylic acids, and their mixtures with salts, is treated  
227 using two different models, namely an extended ZSR ap-  
228 proach, described in *Clegg and Seinfeld* [2004, 2006a] or  
229 the *CSB model*, see *Clegg and Seinfeld* [2006b]; *Clegg*  
230 *et al.* [2004].

231 The first approach to model such interactions is an  
232 extension of the ZSR model as described by *Clegg and*

233 *Seinfeld* [2004]. It uses Pitzer equations to calculate ac-  
 234 tivity coefficients for the inorganic electrolytes and an  
 235 extended ZSR model to evaluate interactions and the  
 236 dissociation of organic solutes. Unfortunately, this ap-  
 237 proach is valid only for fixed concentrations of the dif-  
 238 ferent solutes, which is incompatible with dissociation of  
 239 uncharged solutes and leads to a thermodynamic incon-  
 240 sistency. Therefore the ZSR approach is not used in this  
 241 work.

242 In a second approach, *Clegg and Seinfeld* [2006a] have  
 243 extended the so-called *CSB model*. The activity coeffi-  
 244 cients for the electrolyte and the non-electrolyte organics  
 245 are computed independently, with the PSC and UNIFAC  
 246 models, respectively. Additional terms are then added to  
 247 the activity coefficients with the Pitzer molality-based  
 248 model. We note that the terms in the Pitzer model can  
 249 indeed take unrealistic values in concentrated solutions.

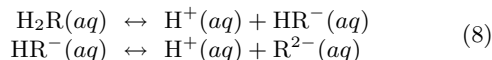
250 Efficient simplifications of these models can improve  
 251 the computational time of UHAERO. The discussion of  
 252 the simplifications of the activity coefficients model is not  
 253 our focus, and therefore we will present results based on  
 254 this standard model.

255 The CSB model is used in the present frame-  
 256 work for the modeling of activity coefficients in inor-  
 257 ganic/dicarboxylic acids mixtures. In this hybrid ther-  
 258 modynamic approach, the molal activity coefficients of  
 259 an ion ( $\gamma_i$ ) and an uncharged organic solute ( $\gamma_n$ ) in a  
 260 liquid mixture are given by:

$$\ln(\gamma_i) = \Delta \ln(\gamma_i[\text{ion-water}]) + \Delta \ln(\gamma_i[\text{ion-organic}]), \quad (6)$$

$$\ln(\gamma_n) = \Delta \ln(\gamma_n[\text{organic-water}]) + \Delta \ln(\gamma_n[\text{ion-organic}]). \quad (7)$$

261 Both activity coefficients have two contributions: one  
 262 incorporating the interactions with water and one incor-  
 263 porating the interactions between electrolytes and organ-  
 264 ics. We illustrate these interactions in the system of sul-  
 265 fate, ammonium, water and one dicarboxylic acid, de-  
 266 noted by  $\text{H}_2\text{R}$ . The stepwise dissociation of the acid is  
 267 given by the following two relations:



268 Owing to a general lack of data, the interactions be-  
 269 tween electrolytes and dissociated acids have been mod-  
 270 eled in a simplified way. The organic ions  $\text{R}^{2-}$  and  $\text{HR}^-$   
 271 are assumed to interact only with the positive inorganic  
 272 ions. The corresponding values of the parameters in the  
 273 model are the same as those for inorganic components  
 274  $\text{SO}_4^{2-}$  and  $\text{HSO}_4^-$ , respectively. The organic ions are as-  
 275 summed not to interact with each other, and the neutral  
 276 organic components  $\text{H}_2\text{R}$  interact only with water.

277 Finally, the inclusion of the PSC and UNIFAC models,  
 278 together with the CSB model for interactions, illustrates  
 279 that the UHAERO framework allows an arbitrary num-  
 280 ber of components with any activity coefficient model.

#### 4. Computation of inorganic electrolyte / organic phase equilibria

281 Minimization algorithms applied for the prediction of  
 282 gas-aerosol equilibrium are often related to sequential  
 283 quadratic programming methods for nonlinear program-  
 284 ming, combined with interior-point techniques for the

285 handling of the non-negativity constraints on the con-  
 286 centrations of salts. When nonlinear programming algo-  
 287 rithms are applied as *black boxes* to solve gas-aerosol  
 288 equilibrium problems, generic linear algebra routines are  
 289 typically employed to solve linear systems arising in the  
 290 algorithm. However, for gas-aerosol equilibrium prob-  
 291 lems, specific sparse direct linear solvers that take ad-  
 292 vantage of the special algebraic structure of gas-liquid  
 293 and liquid-solid equilibrium relations have to be used in  
 294 order to deal with scaling of the concentrations in the  
 295 computation. A straightforward application of nonlinear  
 296 programming algorithms is not effective for such prob-  
 297 lems.

298 The numerical minimization technique of UHAERO,  
 299 described in detail in *Amundson et al.* [2005, 2006b], is  
 300 based on a primal-dual active-set algorithm that takes  
 301 into account the special structure of the underlying sys-  
 302 tem. The algorithm is elucidated from the analysis of the  
 303 algebraic structure of the Karush-Kuhn-Tucker (KKT)  
 304 optimality conditions for the minimization of the Gibbs  
 305 free energy. For a given set of solids  $\bar{\mathcal{I}}_s$  that can occur in  
 306 the system, the KKT optimality conditions are:

$$\begin{aligned} \vec{\mu}_l + A_l^T \lambda &= 0, \\ \vec{\mu}_g + A_g^T \lambda &= 0, \\ \vec{n}_s \geq 0, \quad \vec{\mu}_s + A_s^T \lambda \geq 0, \quad \vec{n}_s^T (\vec{\mu}_s + A_s^T \lambda) &= 0, \\ A_l \vec{n}_l + A_g \vec{n}_g + A_s \vec{n}_s &= \vec{b}. \end{aligned}$$

307 The above KKT system is first reformulated to fur-  
 308 nish the mass action laws in addition to the mass balance  
 309 constraints (2). The mass action laws are expressed in a  
 310 logarithmic form. An immediate consequence of the log-  
 311 arithmic form is that the mass action laws in the primal-  
 312 dual form are linear with respect to the dual variables  
 313  $\lambda$ , which represent the logarithmic values of activities for  
 314 component species at equilibrium. In this primal-dual  
 315 form, the mass action laws involving solid phases be-  
 316 come linear inequality constraints that are enforced via  
 317 the dual variables so that the solution remains dual fea-  
 318 sible with respect to salt saturations. The concentrations  
 319 of saturated salts are the Lagrange multipliers of the dual  
 320 linear constraints that are active, and thus can be elim-  
 321 inated from the KKT system by applying the so-called  
 322 null-space method based on an active set of solid phases.  
 323 The reduced KKT system of equations is obtained by  
 324 projection of the original system on the active set of solid  
 325 salts  $\bar{\mathcal{I}}_s$  and is given by:

$$\begin{aligned} \vec{\mu}_l + A_{z_l}^T \vec{\lambda} &= 0, \\ \vec{\mu}_g + A_{z_g}^T \vec{\lambda} &= 0, \\ A_{z_l} \vec{n}_l + A_{z_g} \vec{n}_g &= \vec{b}, \end{aligned}$$

326 where  $A_{z_l}$  and  $A_{z_g}$  are the matrices  $A_l$  and  $A_g$  premul-  
 327 tiplied by a null-space matrix of the sub-space given by  
 328 the active set of solid salts.

329 Then, the algorithm applies Newton's method to the  
 330 reduced KKT system of equations that is projected on  
 331 the active set of solid phases to find the next primal-  
 332 dual approximation of the solution. The primal-dual al-  
 333 gorithm is based on the active-set strategy that makes  
 334 a sequence of sets  $\bar{\mathcal{I}}_s$  of solids converging to the optimal  
 335 active set  $\bar{\mathcal{I}}_s^\dagger$  of solid phases, *i.e.* the set of solids ex-  
 336 isting at the equilibrium. For each set  $\bar{\mathcal{I}}_s$ , we compute  
 337 the Newton direction. If a solid salt becomes *saturated*,  
 338 we introduce it into the set of active solids and restart  
 339 a Newton method. When the algorithm converges, the  
 340 salts with negative concentrations are removed from the  
 341 active sets of solids salts.

342 The active set method adds a solid salt when the com-  
 343 ponents reach saturation and deletes a solid phase from  
 344 the active set when its concentration violates the non-  
 345 negativity constraint. The analysis of linear algebra with  
 346 matrices of block structure provides information about  
 347 the inertia of the so-called KKT matrices which arise in  
 348 the Newton iterations. This information is used, as phase  
 349 stability criteria, in line-search based methods to modify,  
 350 if necessary, the second order information to ensure that  
 351 the algorithm converges to a stable equilibrium rather  
 352 than to any other first-order optimality point, such as a  
 353 maximum, a saddle point, or an unstable local minimum.  
 354 The concentration iterates follow a path that is not fea-  
 355 sible with respect to the mass balance constraints in the  
 356 first few iterations, but then converge quadratically to  
 357 the minimum of the Gibbs free energy.

358 The addition of organic species to the system does  
 359 not change the underlying mathematical structure of the  
 360 KKT optimality system, but merely increases the number  
 361 of liquid components, the number of chemical reactions,  
 362 and the number of potential salts. In case of a system  
 363 that is equilibrated to a fixed relative humidity ( $RH$ ),  
 364 as the inorganic module described in *Amundson et al.*  
 365 [2006a], the aerosol water content is directly computed  
 366 from the minimization, i.e., without using an empirical  
 367 relationship such as the ZSR equation. Also the equili-  
 368 bration of trace gases between the vapor and condensed  
 369 phases can be enabled or disabled as required, as can the  
 370 formation of solids (which allows the properties of liquid  
 371 aerosols supersaturated with respect to solid phases to  
 372 be investigated).

## 5. Simulation of inorganic electrolytes / dicarboxylic acids phase equilibria

373 The inorganic system that is most widely investigated  
 374 with respect to atmospheric gas-aerosol equilibrium and  
 375 aerosol state is that of sulfate, nitrate, ammonium, and  
 376 water, whose detailed diagrams of phase equilibria have  
 377 been reconstructed in *Amundson et al.* [2006a]. Parti-  
 378 cles consisting of such species can be fully aqueous, fully  
 379 crystalline, or consist of liquid-solid mixtures, depend-  
 380 ing on the relative concentrations of the components,  
 381  $RH$ , and temperature. Global modeling studies using  
 382 inorganic modules can be found for instance in *Adams*  
 383 *et al.* [1999, 2001]; *Ansari and Pandis* [2000]; *Martin*  
 384 [2000]; *Jacobson* [2001]; *Metzger et al.* [2002b]; *Liao et al.*  
 385 [2003, 2004]; *Rodriguez and Dabdub* [2004]; *Kinne et al.*  
 386 [2005]; *Myhre et al.* [2006]; *Tsigaridis et al.* [2006]; *Schulz*  
 387 *et al.* [2006]; *Textor et al.* [2006]; *Bauer et al.* [2006];  
 388 *Luo et al.* [2007]; *Feng and Penner* [2007]; *Metzger and*  
 389 *Lelieveld* [2007]. We focus on the systems consisting  
 390 of sulfate, ammonium, and water together with one di-  
 391 carboxylic acid, such as oxalic, glutaric, malic, malonic,  
 392 maleic and methyl succinic acids, and present results on  
 393 the construction of phase diagrams to exhibit the effect  
 394 of dissociation of the acids.

395 To reconstruct phase diagrams of the system  $\text{SO}_4^{2-} /$   
 396  $\text{NH}_4^+ / \text{H}^+ / \text{H}_2\text{O} / \text{H}_2\text{R}$ , where  $\text{H}_2\text{R}$  denotes the dicar-  
 397 boxylic acid considered, we use composition coordinates  
 398 similar to those introduced in *Amundson et al.* [2006a].  
 399 The total species concentrations can be expressed in  
 400 terms of the coordinates  $(\text{NH}_4)_2\text{SO}_4/\text{H}_2\text{SO}_4/\text{H}_2\text{O}/\text{H}_2\text{R}$   
 401 for convenience:

$$X = \text{Ammonium Fraction} = \frac{b_{\text{NH}_4^+}}{b_{\text{NH}_4^+} + b_{\text{H}^+}} \quad (9)$$

$$= \frac{b_{(NH_4)_2SO_4} + b_{(NH_4)_2R}}{b_{(NH_4)_2SO_4} + b_{(NH_4)_2R} + b_{H_2SO_4} + b_{H_2R}},$$

$$Y = \text{Sulfate Fraction} = \frac{b_{SO_4^{2-}}}{b_{SO_4^{2-}} + b_{R^{2-}}} \quad (10)$$

$$= \frac{b_{(NH_4)_2SO_4} + b_{H_2SO_4}}{b_{(NH_4)_2SO_4} + b_{(NH_4)_2R} + b_{H_2SO_4} + b_{H_2R}}, \quad (11)$$

402 where the concentrations  $b_{SO_4^{2-}}$ ,  $b_{R^{2-}}$ ,  $b_{NH_4^+}$ , and  $b_{H^+}$   
 403 are subject to electro-neutrality. We also define the or-  
 404 ganic fraction  $Y'$  as

$$Y' = \text{Organic Fraction} = \frac{b_{R^{2-}}}{b_{SO_4^{2-}} + b_{R^{2-}}} \quad (12)$$

$$= \frac{b_{H_2SO_4} + b_{H_2R}}{b_{(NH_4)_2SO_4} + b_{(NH_4)_2R} + b_{H_2SO_4} + b_{H_2R}}$$

$$= 1 - Y,$$

### 5.1. Sulfate/Ammonium/Dicarboxylic Acid Systems

405 We present the construction of the phase diagrams at  
 406 298.15 K for systems comprised of sulfate, ammonium,  
 407 water and a dicarboxylic acid ( $H_2R$ ). Six dicarboxylic  
 408 acids are considered and the corresponding phase dia-  
 409 grams are shown, respectively, in Figure 1 (oxalic acid),  
 410 Figure 2 (glutaric acid), Figure 3 (malic acid), Figure 4  
 411 (malonic acid), Figure 5 (maleic acid), and Figure 6  
 412 (methyl succinic acid). As defined earlier, the abscissa  
 413  $X$  is the cation mole fraction arising from  $NH_4^+$ , with  
 414 the remainder coming from  $H^+$ . This can be considered  
 415 as the degree of neutralization of the particle. The or-  
 416 dinate  $Y'$  is the organic mole fraction arising from  $R^{2-}$ ,  
 417 with the balance being made up of  $SO_4^{2-}$ . The phase  
 418 diagrams are therefore represented in the barycentric co-  
 419 ordinates of  $H_2SO_4$  (bottom left),  $(NH_4)_2SO_4$  (bottom  
 420 right) and  $H_2R$  (top). Three possible inorganic solid  
 421 phases exist in the system  $SO_4^{2-} / NH_4^+ / H^+ / H_2O$   
 422  $/ H_2R$ . They are labeled as A through C: A denotes am-  
 423 monium sulfate,  $(NH_4)_2SO_4$  (AS); B denotes letovicite,  
 424  $(NH_4)_3H(SO_4)_2$  (LET); C denotes ammonium bisulfate,  
 425  $NH_4HSO_4$  (AHS). In Figures 1-6, we assume that  $H_2R(s)$   
 426 is the only organic solid that can occur in the system. As  
 427 in *Clegg and Seinfeld* [2006b], the limitations on the set  
 428 of possible dicarboxylate solids treated in the system is a  
 429 result of the lack of available thermodynamic data. The  
 430 first salt to crystallize in system with high organic con-  
 431 centrations is  $H_2R(s)$  in all cases. The threshold for the  
 432 organic fraction that allows the organic salt to crystallize  
 433 first depends on the system considered and of the ammo-  
 434 nium fraction. For a low ammonium fraction, the organic  
 435 salt is crystallizing, while for large ammonium fraction,  
 436 the inorganic salts are still the ones that appear first at  
 437 equilibrium.

438 On each of these figures, horizontal cuts for a given  
 439 organic fraction provide the same kind of results as those  
 440 presented in *Amundson et al.* [2006a].

441 For the sulfate/ammonium/water/succinic acid sys-  
 442 tem, the succinate solids that can occur in the sys-  
 443 tem at 298.15 K are  $H_2Succ(s)$ ,  $NH_4HSucc(s)$ , and  
 444  $(NH_4)_2Succ \cdot H_2O(s)$ . Figures 7 and 8 illustrate the  
 445 phase diagrams of the system in the absence and pres-  
 446 ence of the two additional salts  $NH_4HSucc(s)$ , and  
 447  $(NH_4)_2Succ \cdot H_2O(s)$ . The abscissa  $X$  and the ordi-  
 448 nate  $Y'$  are the same as before. The phase diagrams  
 449 are represented in the barycentric coordinates of  $H_2Succ$   
 450 (top left),  $(NH_4)_2Succ$  (top right),  $H_2SO_4$  (bottom left),

451 (NH<sub>4</sub>)<sub>2</sub>SO<sub>4</sub> (bottom right). One can observe that the  
452 topology changes in the phase diagrams owing to the  
453 presence of the additional two salts. The addition of the  
454 two salts NH<sub>4</sub>HSucc(s), and (NH<sub>4</sub>)<sub>2</sub>Succ · H<sub>2</sub>O(s) does  
455 not alter the lower left part of the phase diagram. On the  
456 other hand, the influence of organic solids is clear for the  
457 upper right part. Therefore the incorporation of organic  
458 salts is crucial in the modeling of hygroscopicity prop-  
459 erties as well as multistage growth of organic/inorganic  
460 mixtures.

461 In Figures 1–8, regions outlined by heavy black lines  
462 show the first solid that reaches saturation with decreas-  
463 ing *RH*. The thin labeled solid lines are deliquescence  
464 relative humidity contours, and the dotted lines give the  
465 aqueous-phase *X-Y'* composition variation with decreas-  
466 ing relative humidity as more solid crystallizes. These so-  
467 called liquidus lines have been introduced by *Potukuchi*  
468 *and Wealer* [1995].

469 In order to validate the UHAERO model and observe  
470 the influence of the activity coefficient model, the ExU-  
471 NIQUAC model described in *Thomsen and Rasmussen*  
472 [1999] is used to replace the PSC model. The param-  
473 eters for H<sub>2</sub>O, H<sup>+</sup>, NH<sub>4</sub><sup>+</sup>, SO<sub>4</sub><sup>2-</sup> and HSO<sub>4</sub><sup>-</sup> are taken from  
474 *Thomsen and Rasmussen* [1999]. In this work, volume  
475 and surface area parameters, *r* and *q*, for the organic  
476 ions R<sup>2-</sup> and HR<sup>-</sup> and parameters for the interaction  
477 between water and the organic ions R<sup>2-</sup> and HR<sup>-</sup> and  
478 between the organic ions R<sup>2-</sup> and HR<sup>-</sup> and the positive  
479 inorganic ions are assumed to be the same as those for in-  
480 organic components SO<sub>4</sub><sup>2-</sup> and HSO<sub>4</sub><sup>-</sup>, respectively. The  
481 organic ions are assumed not to interact with each other,  
482 and the neutral organic components H<sub>2</sub>R interact only  
483 with water.

484 Figure 9 shows the phase diagram reconstructed with  
485 the ExUNIQUAC model for the sulfate/ammonium/glutaric  
486 acid system. Compared to the phase diagram recon-  
487 structed with the PSC model as illustrated in Figure 2,  
488 one can observe that the two phase diagrams have iden-  
489 tical topological phase structures. Differences in the *RH*  
490 values at which the first salt crystallizes are mostly con-  
491 fined to the H<sub>2</sub>SO<sub>4</sub> corner region of the phase diagrams.

492 Efflorescence and hysteresis for mixtures of inorganic  
493 and organic species can be modeled with UHAERO in  
494 a similar fashion as in *Amundson et al.* [2006a] for pure  
495 inorganic systems.

496 Extensions of the model, in terms of hydrated salt  
497 compounds or crustal species as in *Fountoukis and Nenes*  
498 [2007] or *Metzger and Lelieveld* [2007] can be consid-  
499 ered in the future. To that extent, the limitations of the  
500 UHAERO framework are those of the activity coefficient  
501 model.

## 5.2. Computational efficiency

502 The UHAERO module can be run in two modes, de-  
503 pending on the circumstances of its application. The so-  
504 called *cold start* mode is used when no information on  
505 the system is available *a priori*. The system is therefore  
506 initialized as an infinitely dilute solution. The so-called  
507 *warm-start* mode initializes the system with the conver-  
508 gent solution at a neighboring state. The latter case is  
509 the one relevant in a 3-D chemical transport model when  
510 using the convergent solution at the previous time step.  
511 The computational cost of the inorganic module has been  
512 discussed in *Amundson et al.* [2006b]. We present here  
513 results for the computational cost of UHAERO, with the  
514 PSC model for the activity coefficients of inorganic elec-  
515 trolytes and when the warm-start strategy is applied, for  
516 the reconstruction of the phase diagrams presented in  
517 Subsection 5.1.

518 The calculations are performed on a Linux PC  
519 equipped with Intel(R) Pentium(R) 4 3.20 GHz proces-  
520 sor. The tolerance for stopping the iterations is set to  
521  $10^{-8}$ , *i.e.* the residuals for both the mass balances and  
522 the liquid mass action laws are set to be less than  $10^{-8}$   
523 in absolute value.

524 Let us consider first the case of fixed water content cal-  
525 culations. For the system involving a dicarboxylic acid,  
526 an average number of 3.5 Newton iterations per grid point  
527 is required for the convergence solution, with an average  
528 CPU-time of 49.5  $\mu$ s per Newton iteration. The com-  
529 putational time can be split into the activity coefficient  
530 calculations and the solution of the nonlinear system.  
531 The average CPU-percentage per Newton iteration for  
532 activity coefficient calculations is 75.0%. For the system  
533 without dicarboxylic acids (*i.e.*, the sulfate-ammonium-  
534 water system), an average number of 3.0 Newton itera-  
535 tions per grid point is needed for the convergence solution  
536 with an average CPU-time of 24.7  $\mu$ s per iteration. The  
537 average CPU-percentage per Newton iteration for activ-  
538 ity coefficient calculations is 64.3%. One can conclude  
539 that the addition of dicarboxylic acids does not increase  
540 the average number of iterations per grid point, but that  
541 each iteration is approximately twice as costly in terms  
542 of CPU-times.

543 Let us now compare the calculations with fixed *RH*.  
544 For the system involving a dicarboxylic acid, an average  
545 number of 3.7 Newton iterations per grid point is required  
546 for the convergence solution with an average CPU-time of  
547 71.7  $\mu$ s per Newton iteration. The computation of the ac-  
548 tivity coefficients takes 71.2 % of the total computational  
549 time. For the system without dicarboxylic acid (*i.e.*, the  
550 sulfate-ammonium-water system), an average number of  
551 3.3 Newton iterations per grid point is needed for the con-  
552 vergent solution with an average CPU-time of 35.3  $\mu$ s per  
553 iteration. The average CPU-percentage per Newton itera-  
554 tion for activity coefficient calculations is 67.4 %. Again,  
555 the addition of dicarboxylic acids does not increase the  
556 average number of iterations, but again each iteration is  
557 approximately twice as expensive in terms of CPU-times.

558 We can draw two conclusions. First, the computa-  
559 tional effort required to calculate the equilibrium state  
560 in addition to the calculation of the activity coefficient is  
561 small (the major fraction of the time being the evalua-  
562 tion of the accurate model for the activity coefficients).  
563 Secondly, the additional computational effort to take into  
564 account the organic components with respect to the in-  
565 organic code presented in *Amundson et al.* [2006a] does  
566 not change the number of iterations but the cost of each  
567 iteration is increased. In the light of these results, the  
568 overall computational performance of UHAERO depends  
569 significantly on the efficiency and precision of the activity  
570 coefficient model. The computational time used for the  
571 evaluation of the activity coefficients could be reduced by  
572 considering simpler models.

## 6. Conclusions

573 A new version of the phase equilibrium model for at-  
574 mospheric aerosols for mixtures of inorganic electrolytes  
575 and organic compounds has been introduced. Model-  
576 ing results are presented for the phase behavior in the  
577 sulfate/ammonium/water/dicarboxylic acid system, us-  
578 ing the Pitzer-Simonson-Clegg (PSC) and UNIFAC ac-  
579 tivity coefficient models, together with a CSB approach  
580 for the modeling of interactions between inorganic elec-  
581 trolytes and organic dissociated components. Sensitivity  
582 analysis has been performed by using the ExUNQUAC  
583 activity coefficient model in place of the PSC model for

584 the inorganic compounds.

585 The UHAERO code has been prepared so that it may  
586 be easily used as a computational framework by the com-  
587 munity.

588 **Acknowledgments.** This research has been supported  
589 by U.S. Environmental Protection Agency grant X-83234201.  
590 The authors thank S. L. Clegg for providing the data for the  
591 CSB model based activity coefficient calculation. The second  
592 author is partially supported by University of Houston New  
593 Faculty Grant.

## References

- 594 Adams, P. J., J. H. Seinfeld, and D. M. Koch (1999), Global  
595 concentrations of tropospheric sulfate, nitrate, and am-  
596 monium aerosol simulated in a general circulation model,  
597 *Journal of Geophysical Research*, *104*, 13,791–13,823.
- 598 Adams, P. J., J. H. Seinfeld, D. Koch, L. Mickley, and D. Jacob  
599 (2001), General circulation model assessment of direct ra-  
600 diative forcing by the sulfate-nitrate-ammonium-water in-  
601 organic aerosol system, *Journal of Geophysical Research*,  
602 *106*(D1), 10977-1112.
- 603 Amundson, N. R., A. Caboussat, J. W. He, J. H. Seinfeld, and  
604 K.-Y. Yoo (2005), An optimization problem related to the  
605 modeling of atmospheric inorganic aerosols, *C. R. Acad.*  
606 *Sci. Paris, Ser. I*, *340*(9), 683–686.
- 607 Amundson, N. R., A. Caboussat, J. W. He, A. V. Martynenko,  
608 V. B. Savarin, J. H. Seinfeld, and K.-Y. Yoo (2006a), A  
609 new inorganic atmospheric aerosol phase equilibrium model  
610 (UHAERO), *Atmos. Chem. Phys.*, *6*, 975–992.
- 611 Amundson, N. R., A. Caboussat, J. W. He, J. H. Seinfeld,  
612 and K.-Y. Yoo (2006b), Primal-dual active-set algorithm  
613 for chemical equilibrium problems related to the modeling  
614 of atmospheric inorganic aerosols, *Journal of Optimization*  
615 *Theory and Applications*, *128*(3), 469–498.
- 616 Ansari, A. S., and S. N. Pandis (1999), Prediction of multi-  
617 component inorganic atmospheric aerosol behavior, *Atmos.*  
618 *Environ.*, *33*, 745–757.
- 619 Ansari, A. S., and S. N. Pandis (2000), The effect of metastable  
620 equilibrium states on the partitioning of nitrate between the  
621 gas and aerosol phases, *Atmospheric Environment*, *34*(1),  
622 157–168.
- 623 Bassett, M., and J. H. Seinfeld (1983), Atmospheric equilib-  
624 rium model of sulfate and nitrate aerosol, *Atmospheric En-*  
625 *vironment*, *17*, 2237–2252.
- 626 Bassett, M., and J. H. Seinfeld (1984), Atmospheric equilib-  
627 rium model of sulfate and nitrate aerosols-II. particle size  
628 analysis, *Atmospheric Environment*, *18*, 1163–1170.
- 629 Bauer, S., M. I. Mishchenko, A. A. Lacis, S. Zhang, J. Perl-  
630 witz, and S. M. Metzger (2006), Radiative properties of  
631 ammonium sulfate and nitrate coated mineral dust, *J Geo-*  
632 *phys. Res.*, *in press*.
- 633 Binkowski, F., and U. Shankar (1995), The regional particu-  
634 late matter model, 1: model description and preliminary  
635 results, *J. of Geophysical Research*, *100*, 26,191–26,209.
- 636 Clegg, S. L., and K. S. Pitzer (1992), Thermodynamics  
637 of multicomponent, miscible, ionic solutions: generalized  
638 equations for symmetrical electrolytes, *Journal of Physical*  
639 *Chemistry*, *96*(8), 3513 – 3520.
- 640 Clegg, S. L., and J. H. Seinfeld (2004), Improvement of the  
641 Zdanovskii-Stokes-Robinson model for mixtures containing  
642 solutes of different charge types, *Journal of Physical Chem-*  
643 *istry*, *108*(6), 1008 –1017.
- 644 Clegg, S. L., and J. H. Seinfeld (2006a), Thermodynamic mod-  
645 els of aqueous solutions containing electrolytes and dicar-  
646 boxylic acids at 298.15 K 1. the acids as nondissociating  
647 components, *J. Phys. Chem.*, *110*, 5692–5717.
- 648 Clegg, S. L., and J. H. Seinfeld (2006b), Thermodynamic mod-  
649 els of aqueous solutions containing electrolytes and dicar-  
650 boxylic acids at 298.15 K 2. systems including dissociation  
651 equilibria, *J. Phys. Chem.*, *110*, 5718–5734.
- 652 Clegg, S. L., K. S. Pitzer, and P. Brimblecombe (1992), Ther-  
653 modynamics of multicomponent, miscible, ionic solutions.

654 mixtures including unsymmetrical electrolytes, *Journal of*  
655 *Physical Chemistry*, 96(23), 9470–9.

656 Clegg, S. L., P. Brimblecombe, and A. S. Wexler (1998a),  
657 Thermodynamic model of the system  $\text{H}^+\text{-NH}_4^+\text{-SO}_4^{2-}\text{-}$   
658  $\text{NO}_3^-\text{-H}_2\text{O}$  at tropospheric temperatures, *Journal of Phys-*  
659 *ical Chemistry A*, 102(12), 2137–2154.

660 Clegg, S. L., P. Brimblecombe, and A. S. Wexler (1998b),  
661 Thermodynamic model of the system  $\text{H}^+\text{-NH}_4^+\text{-Na}^+\text{-}$   
662  $\text{SO}_4^{2-}\text{-NO}_3^-\text{-Cl}^-\text{-H}_2\text{O}$  at 298.15 K, *J. Phys. Chem.*, 102,  
663 2155–2171.

664 Clegg, S. L., J. H. Seinfeld, and E. O. Edney (2003), Ther-  
665 modynamic modelling of aqueous aerosols containing elec-  
666 trolytes and dissolved organic compounds. II. an extended  
667 Zdanovskii-Stokes-Robinson approach, *Journal of Aerosol*  
668 *Science*, 34(6), 667–690.

669 Clegg, S. L., J. H. Seinfeld, and P. Brimblecombe (2004), Ther-  
670 modynamic modelling of aqueous aerosols containing elec-  
671 trolytes and dissolved organic compounds., *J. Aerosol. Sci.*,  
672 32, 713–738.

673 Erdakos, G. B., and J. F. Pankow (2004), Gas/particle parti-  
674 tioning of neutral and ionizing compounds to single- and  
675 multi-phase aerosol particles. 2. phase separation in liq-  
676 uid particulate matter containing both polar and low-  
677 polarity organic compounds, *Atmospheric Environment*,  
678 38(7), 1005–1013.

679 Feng, Y., and J. E. Penner (2007), Global modeling of nitrate  
680 and ammonium: Interaction of aerosols and tropospheric  
681 chemistry, *Journal of Geophysical Research*, 112, D01,304,  
682 doi:10.1029/2005JD006404.

683 Fountoukis, C., and A. Nenes (2007), ISORROPIA II: a com-  
684 putationally efficient thermodynamic equilibrium model for  
685  $\text{K}^+\text{-Ca}^{2+}\text{-Mg}^{2+}\text{-NH}_4^+\text{-Na}^+\text{-SO}_4^{2-}\text{-NO}_3^-\text{-Cl}^-\text{-H}_2\text{O}$  aerosols,  
686 *Atmos. Chem. Phys., Discuss.*, 7, 1893–1939.

687 Fredenslund, A., J. Gmehling, and P. Rasmussen (1977),  
688 *Vapor-Liquid Equilibrium Using UNIFAC*, Elsevier, Am-  
689 sterdam.

690 Griffin, R. J., D. Dabdub, and J. H. Seinfeld (2005), De-  
691 velopment and initial evaluation of a dynamic species-  
692 resolved model for gas-phase chemistry and size-resolved  
693 gas/particle partitioning associated with secondary organic  
694 aerosol formation, *Journal of Geophysical Research*, 110,  
695 D05,304.

696 Jacobson, M. (1999), Simulating equilibrium within aerosols  
697 and nonequilibrium between gases and aerosols, *Atmos.*  
698 *Env.*, 30, 3635–3649.

699 Jacobson, M., A. Tabazadeh, and R. Turco (1996), Simu-  
700 lating equilibrium within aerosols and nonequilibrium be-  
701 tween gases and aerosols, *Journal of Geophysical Research*,  
702 101(D4), 9079–9091.

703 Jacobson, M. Z. (2001), Global direct radiative forcing due to  
704 multicomponent anthropogenic and natural aerosols, *Jour-*  
705 *nal of Geophysical Research*, 106, 1551–1568.

706 Kawamura, K., N. Umemoto, M. Mochida, T. Bertram,  
707 S. Howell, and B. J. Huebert (2003), Water-soluble dicar-  
708 boxylic acids in the tropospheric aerosols collected over east  
709 asia and western north pacific by ACE-asia C-130 aircraft,  
710 *J. Geophys. Res.*, 108(D23), 8639.

711 Kim, Y. P., and J. H. Seinfeld (1995), Atmospheric gas-aerosol  
712 equilibrium III. thermodynamics of crustal elements  $\text{Ca}^{2+}$ ,  
713  $\text{K}^+$ , and  $\text{Mg}^{2+}$ , *Aerosol Science and Technology*, 22, 93–  
714 110.

715 Kim, Y. P., J. H. Seinfeld, and P. Saxena (1993a), Atmospheric  
716 gas-aerosol equilibrium I. thermodynamic model, *Aerosol*  
717 *Science and Technology*, 19, 157–181.

718 Kim, Y. P., J. H. Seinfeld, and P. Saxena (1993b), Atmo-  
719 spheric gas-aerosol equilibrium II. analysis of common ap-  
720 proximations and activity coefficient calculation methods,  
721 *Aerosol Science and Technology*, 19, 182–198.

722 Kinne, S., M. Schulz, C. Textor, S. Guibert, Y. Balkanski,  
723 S. E. Bauer, T. Berntsen, T. F. Berglen, O. Boucher,  
724 M. Chin, W. Collins, F. Dentener, T. Diehl, R. Easter,  
725 J. Feichter, D. Fillmore, S. Ghan, P. Ginoux, S. Gong,  
726 A. Grini, J. Hendricks, M. Herzog, L. Horowitz, I. Isaksen,  
727 T. Iversen, A. Kirkevg, S. Kloster, D. Koch, J. E. Krist-  
728 jansson, M. Krol, A. Lauer, J. F. Lamarque, G. Lesins,  
729 X. Liu, U. Lohmann, V. Montanaro, G. Myrhe, J. Pen-

ner, G. Pitari, S. Reddy, O. Seland, P. Stier, T. Takemura,  
and X. Tie (2005), An aerocom initial assessment – optical  
properties in aerosol component modules of global models,  
*Atmos. Chem. Phys. Discuss.*, *5*(5), 8285–8330.

Liao, H., P. J. Adams, S. H. Chung, J. H. Seinfeld, L. J. Mick-  
ley, and D. J. Jacob (2003), Interactions between tropo-  
spheric chemistry and aerosols in a unified general circula-  
tion model, *Journal of Geophysical Research*, *108*, D14,001,  
doi:10.1029/2001JD001260.

Liao, H., J. H. Seinfeld, P. J. Adams, and L. J. Mick-  
ley (2004), Global radiative forcing of coupled tropo-  
spheric ozone and aerosols in a unified general circulation  
model, *Journal of Geophysical Research*, *109*, D16,207, doi:  
10.1029/2003JD004456.

Luo, C., C. S. Zender, H. Brian, and S. Metzger (2007), Role  
of ammonia chemistry and coarse mode aerosols in global  
climatological inorganic aerosol distributions, *Atmos. Environ.*,  
*41*(12), 2510–2533.

Makar, P. A., V. S. Bouchet, and A. Nenes (2003), In-  
organic chemistry calculations using HETV - vectorized  
solver for  $\text{SO}_4^{2-}/\text{NO}_3^-/\text{NH}_4^+$  system based on the ISOR-  
ROPIA algorithms, *Atmos. Environ.*, *37*(16), 2279–2294,  
doi:10.1016/S1352-2310(03)00074-8.

Marculli, C., and U. K. Krieger (2006), Phase changes during  
hygroscopic cycles of mixed organic/inorganic model sys-  
tems of tropospheric aerosols, *J. Phys. Chem.*, *110*, 1881–  
1893.

Martin, S. T. (2000), Phase transitions of aqueous atmospheric  
particles, *Chemical Reviews*, *100*(9), 3403–3454.

Meng, Z. Y., J. H. Seinfeld, P. Saxena, and Y. P. Kim (1995),  
Atmospheric gas-aerosol equilibrium IV. thermodynamics  
of carbonates, *Aerosol Science and Technology*, *23*, 131–  
154.

Metzger, S., and J. Lelieveld (2007), Reformulating atmo-  
spheric aerosol thermodynamics and hygroscopic growth  
into haze and clouds, *Atmos. Chem. Phys., Discuss.*, *7*, 849–  
910.

Metzger, S., F. Dentener, S. Pandis, and J. Lelieveld (2002a),  
Gas/aerosol partitioning: 1. a computationally efficient  
model, *Journal of Geophysical Research*, *107*(D16), 4312,  
doi:10.1029/2001JD001102.

Metzger, S., F. Dentener, M. Krol, A. Jeurken, and J. Lelieveld  
(2002b), Gas/aerosol partitioning - 2. global modeling re-  
sults, *Journal of Geophysical Research*, *107*(D16), 4313,  
doi:10.1029/2001JD001103.

Metzger, S., N. Mihalopoulos, and J. Lelieveld (2006), Impor-  
tance of mineral cations and organics in gas-aerosol parti-  
tioning of reactive nitrogen compounds: case study based  
on MINOS results, *Atmos. Chem. Phys.*, *6*, 2549–2567.

Myhre, G., A. Grini, and S. Metzger (2006), Modelling of  
nitrate and ammonium-containing, aerosols in presence of  
sea salt, *Atmos. Chem. Phys.*, *6*, 4809–4821.

Nenes, A., S. N. Pandis, and C. Pilinis (1998), ISORROPIA:  
A new thermodynamic equilibrium model for multiphase  
multicomponent inorganic aerosols, *Aquatic Geochemistry*,  
*4*, 123–152.

Pilinis, C., and J. Seinfeld (1987), Continued development of  
a general equilibrium model for inorganic multicomponent  
atmospheric aerosols, *Atmospheric Environment*, *21*, 2453–  
2466.

Pilinis, C., K. P. Capaldo, A. Nenes, and S. N. Pandis (2000),  
Madm - a new multicomponent aerosol dynamics model,  
*Aerosol Sci. Tech.*, *32*(5), 482–502.

Pitzer, K. S. (1973), Thermodynamics of electrolytes 1. the-  
oretical basis and general equations, *J. Phys. Chem.*, *77*,  
268–277.

Pitzer, K. S. (1975), Thermodynamics of electrolytes 5. effects  
of higher-order electrostatic terms, *J. Solution Chem.*, *4*,  
249–265.

Pitzer, K. S., and G. Mayorga (1973), Thermodynamics of  
electrolytes, 2. activity and osmotic coefficients for strong  
electrolytes with one or both ions univalent, *J. Phys.  
Chem.*, *77*, 2300–2308.

Potukuchi, S., and A. S. Wexler (1995), Identifying solid-  
aqueous-phase transitions in atmospheric aerosols. II. acidic  
solutions, *Atmos. Environ.*, *29*, 3357–3364.

806 Pun, B., R. Griffin, C. Seigneur, and J. Seinfeld (2002),  
807 Secondary organic aerosol: 2. thermodynamic model for  
808 gas/particle partitioning of molecular constituents., *Journal*  
809 *of Geophysical Research*, *107*, AAC4/1–AAC4/15.

810 Rodriguez, M., and D. Dabdub (2004), IMAGES-SCAPE2: A  
811 modeling study of size and chemically resolved aerosol ther-  
812 modynamics in a global chemical transport model, *Journal*  
813 *of Geophysical Research*, *109*, D02,203.

814 Salcedo, D. (2006), Equilibrium phase diagrams of aqueous  
815 mixtures of malonic acid and sulfate/ammonium salts, *J.*  
816 *Phys. Chem., Part A, to appear*, doi:10.1021/jp063850v.

817 Saxena, P., H. A. B., C. Seigneur, and J. H. Seinfeld (1986), A  
818 comparative study of equilibrium approaches to the chemi-  
819 cal characterization of secondary aerosols, *Atmospheric En-*  
820 *vironment*, *20*, 1471–1483.

821 Schulz, M., C. Textor, S. Kinne, Y. Balkanski, S. Bauer,  
822 T. Bertsen, T. Berglen, O. Boucher, F. Dentener, S. Guib-  
823 ert, I. S. A. Isaksen, T. Iversen, D. Koch, A. Kirkev-  
824 g, X. Liu, V. Montanaro, G. Myrhe, J. E. Penner, G. Pitari,  
825 S. Reddy, O. Seland, P. Stier, and T. Takemura (2006),  
826 Radiative forcing by aerosols as derived from the aerocom  
827 present-day and pre-industrial simulations, *Atmos. Chem.*  
828 *Phys. Discuss.*, *6*(3), 5095–5136.

829 Stokes, R. H., and R. A. Robinson (1966), Interactions in aque-  
830 ous nonelectrolyte solutions, I. solute-solvent equilibria, *J.*  
831 *Phys. Chem.*, *70*, 2126–2131.

832 Textor, C., M. Schulz, S. Guibert, S. Kinne, Y. Balkanski,  
833 S. Bauer, T. Bernsten, T. Berglen, O. Boucher, M. Chin,  
834 F. Dentener, T. Diehl, R. Easter, H. Feichter, D. Fill-  
835 more, S. Ghan, P. Ginoux, S. Gong, A. Grini, J. Hen-  
836 dricks, L. Horowitz, P. Huang, I. Isaksen, T. Iversen,  
837 S. Kloster, D. Koch, A. Kirkevag, J. E. Kristjansson,  
838 M. Krol, A. Lauer, J. F. Lamarque, X. Liu, V. Monta-  
839 naro, and G. Myhre (2006), Analysis and quantification of  
840 the diversities of aerosol life cycles within aerocom, *Atmos.*  
841 *Chem. Phys.*, *6*, 1777–1813.

842 Thomsen, K., and P. Rasmussen (1999), Modeling of vapor-  
843 liquid-solid equilibrium in gas-aqueous electrolyte systems,  
844 *Chem. Eng. Sci.*, *54*, 1787–1802.

845 Topping, D. O., G. B. McFiggans, and H. Coe (2005a),  
846 A curved multi-component aerosol hygroscopicity model  
847 framework: Part 1 - inorganic compounds, *Atmospheric*  
848 *Chemistry and Physics*, *5*, 1205–1222.

849 Topping, D. O., G. B. McFiggans, and H. Coe (2005b),  
850 A curved multi-component aerosol hygroscopicity model  
851 framework: Part 2 : Including organic compounds, *Atmo-*  
852 *spheric Chemistry and Physics*, *5*, 1223–1242.

853 Trebs, I., S. Metzger, F. X. Meixner, G. Helas, A. Hof-  
854 fer, Y. Rudich, A. H. Falkovich, M. A. L. Moura, R. S.  
855 da Silva Jr., P. Artaxo, J. Slanina, and M. O. Andreae  
856 (2005), The  $\text{NH}_4^+$ - $\text{NO}_3^-$ - $\text{Cl}^-$ - $\text{SO}_4^{2-}$ - $\text{H}_2\text{O}$  aerosol system  
857 and its gas phase precursors at a pasture site in the ama-  
858 zon basin: How relevant are mineral cations and solu-  
859 ble organic acids?, *J. Geophys. Res.*, *110*, D07,303, doi:  
860 10.1029/2004JD005478.

861 Tsigaridis, K., M. Krol, F. J. Dentener, Y. Balkanski, J. Lath-  
862 iere, S. Metzger, D. A. Hauglustaine, and M. Kanakidou  
863 (2006), Change in global aerosol composition since prein-  
864 dustrial times, *Atmos. Chem. Phys.*, *6*, 5143–5162.

865 Wexler, A. S., and S. L. Clegg (2002), Atmospheric aerosol  
866 models for systems including the ions  $\text{H}^+$ ,  $\text{NH}_4^+$ ,  $\text{Na}^+$ ,  
867  $\text{SO}_4^{2-}$ ,  $\text{NO}_3^-$ ,  $\text{Cl}^-$ ,  $\text{Br}^-$ , and  $\text{H}_2\text{O}$ , *Journal of Geophys-*  
868 *ical Research*, *107*(D14), 4207, doi:10.1029/2001JD000451.

869 Yu, L. E., M. L. Shulman, R. Kopperud, and L. M. Hildemann  
870 (2005), Characterization of organic compounds collected  
871 during southeastern aerosol and visibility study: Water-  
872 soluble organic species, *Environ. Sci. Technol.*, *39*(3), 707–  
873 715.

874 Zaveri, R. A., R. C. Easter, and L. K. Peters (2005a), A com-  
875 putationally efficient multicomponent equilibrium solver for  
876 aerosols (MESA), *Journal of Geophysical Research*, *110*,  
877 D24,203.

878 Zaveri, R. A., R. C. Easter, and A. S. Wexler (2005b),  
879 A new method for multicomponent activity coefficients of  
880 electrolytes in aqueous atmospheric aerosols, *Journal of*  
881 *Geophysical Research*, *110*, D02,201, doi:  
882 10.1029/2004JD004681.

883 Zhang, Y., C. Seigneur, J. H. Seinfeld, M. Jacobson, S. L.  
884 Clegg, and F. S. Binkowski (2000), A comparative review  
885 of inorganic aerosol thermodynamic equilibrium modules:  
886 similarities, differences, and their likely causes, *Atmos. En-*  
887 *viron.*, *34*(1), 117–137.

\_\_\_\_\_

888 N. R. Amundson, Department of Mathematics, University  
889 of Houston, 4800 Calhoun Rd, Houston, TX 77204-3008, USA.  
890 (amundson@uh.edu)

891 A. Caboussat, Department of Mathematics, University of  
892 Houston, 4800 Calhoun Rd, Houston, TX 77204-3008, USA.  
893 (caboussat@math.uh.edu)

894 J. W. He, Department of Mathematics, University of Hous-  
895 ton, 4800 Calhoun Rd, Houston, TX 77204-3008, USA. (ji-  
896 wenhe@math.uh.edu)

897 A. V. Martynenko, Department of Mathematics, University  
898 of Houston, 4800 Calhoun Rd, Houston, TX 77204-3008, USA.  
899 (andrey@math.uh.edu)

900 J. H. Seinfeld, Department of Chemical Engineering, Cal-  
901 ifornia Institute of Technology, Pasadena, CA 91125, USA.  
902 (seinfeld@caltech.edu)

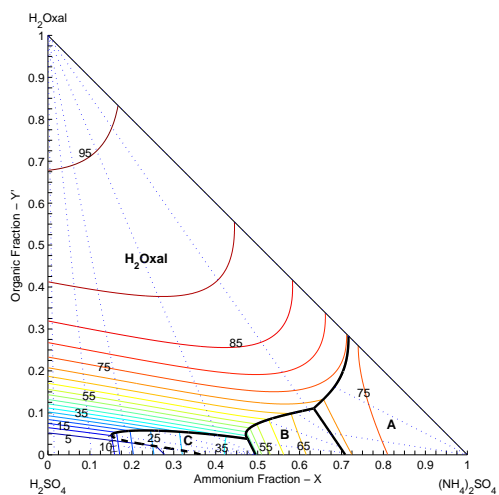


**Figure 1.** Construction of the sulfate/ammonium/oxalic acid ( $\text{H}_2\text{Oxal}$ ) phase diagram at 298.15 K with tracking of the presence of each solid phase. For each region of space whose boundaries are marked with bold lines, the solid phase at equilibrium is represented. Labels on the contours present the Relative Humidity.

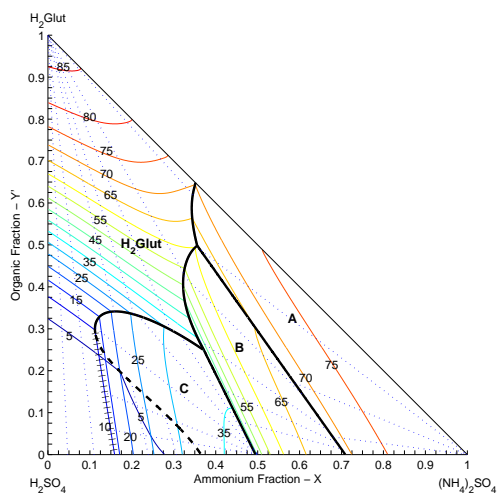


**Figure 2.** Construction of the sulfate/ammonium/glutaric acid ( $\text{H}_2\text{Glut}$ ) phase diagram at 298.15 K with tracking of the presence of each solid phase. For each region of space whose boundaries are marked with bold lines, the solid phase at equilibrium is represented. Labels on the contours present the Relative Humidity.

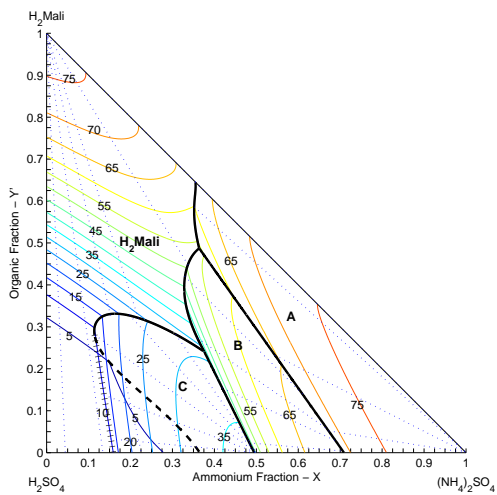


**Figure 3.** Construction of the sulfate/ammonium/malic acid ( $H_2Mali$ ) phase diagram at 298.15 K with tracking of the presence of each solid phase. For each region of space whose boundaries are marked with bold lines, the solid phase at equilibrium is represented. Labels on the contours present the Relative Humidity.

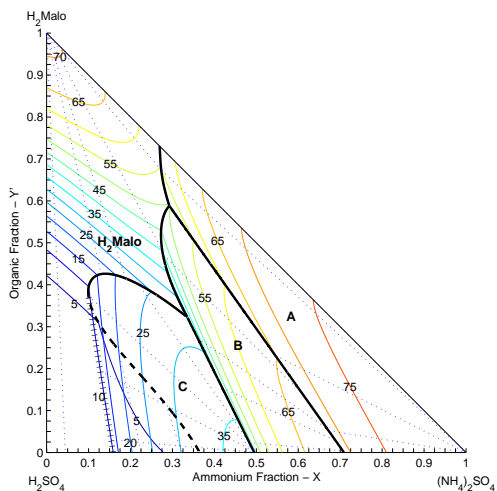


**Figure 4.** Construction of the sulfate/ammonium/malonic acid ( $H_2Malo$ ) phase diagram at 298.15 K with tracking of the presence of each solid phase. For each region of space whose boundaries are marked with bold lines, the solid phase at equilibrium is represented. Labels on the contours present the Relative Humidity.

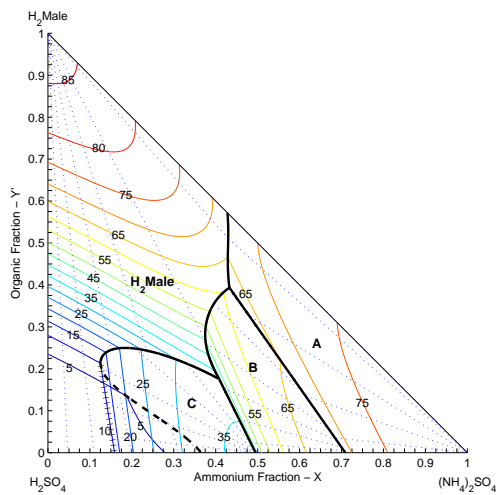


**Figure 5.** Construction of the sulfate/ammonium/maleic acid ( $H_2$ Maleic) phase diagram at 298.15 K with tracking of the presence of each solid phase. For each region of space whose boundaries are marked with bold lines, the solid phase at equilibrium is represented. Labels on the contours present the Relative Humidity.

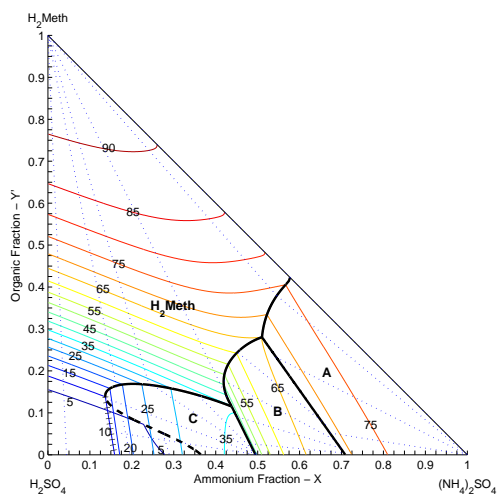


**Figure 6.** Construction of the sulfate/ammonium/methyl succinic acid ( $H_2$ Meth) phase diagram at 298.15 K with tracking of the presence of each solid phase. For each region of space whose boundaries are marked with bold lines, the solid phase at equilibrium is represented. Labels on the contours present the Relative Humidity.

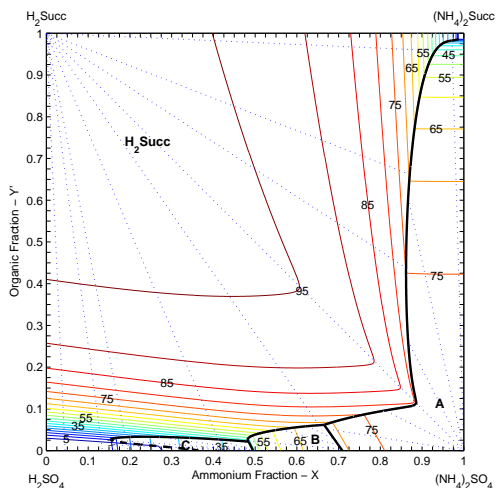


**Figure 7.** Construction of the sulfate/ammonium/succinic acid ( $\text{H}_2\text{Succ}$ ) phase diagram at 298.15 K with tracking of the presence of each solid phase.  $\text{H}_2\text{Succ}(\text{s})$  is the only succinate solid that is modeled. For each region of space whose boundaries are marked with bold lines, the solid phase at equilibrium is represented. Labels on the contours present the Relative Humidity.

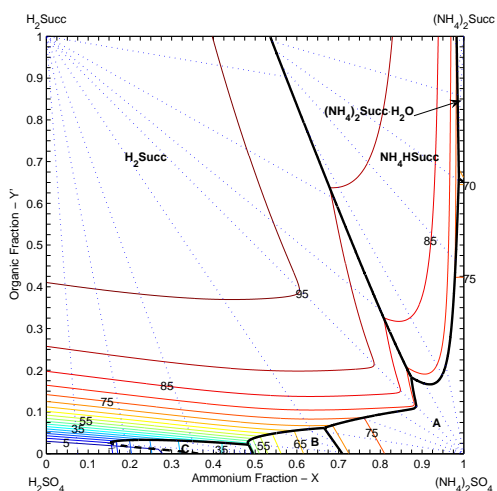


**Figure 8.** Construction of the sulfate/ammonium/succinic acid ( $\text{H}_2\text{Succ}$ ) phase diagram at 298.15 K with tracking of the presence of each solid phase. The succinate solids that can occur in the system are  $\text{H}_2\text{Succ}(\text{s})$ ,  $\text{NH}_4\text{HSucc}(\text{s})$ , and  $(\text{NH}_4)_2\text{Succ} \cdot \text{H}_2\text{O}(\text{s})$ . For each region of space whose boundaries are marked with bold lines, the solid phase at equilibrium is represented. Labels on the contours present the Relative Humidity.

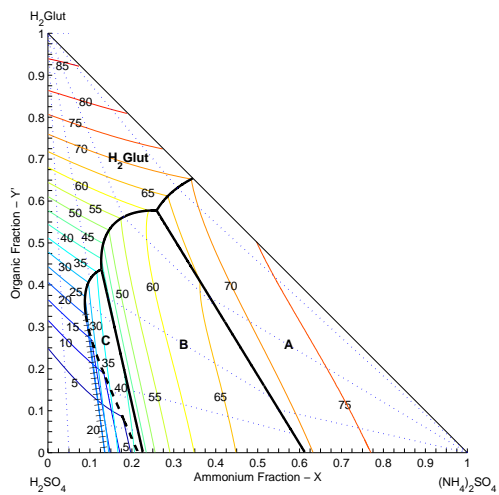


**Figure 9.** Construction of the sulfate/ammonium/glutaric acid ( $\text{H}_2\text{Glut}$ ) phase diagram at 298.15 K with tracking of the presence of each solid phase. The model for the activity coefficients for the inorganic electrolytes is the ExUNIQUAC model. For each region of space whose boundaries are marked with bold lines, the solid phase at equilibrium is represented. Labels on the contours present the Relative Humidity.